CMLS Cellular and Molecular Life Sciences

Structure of angiotensin I-converting enzyme

E. D. Sturrock[a], R. Natesh[b], J. M. van Rooyen[a] and K. R. Acharya[b,*]

[a] Division of Medical Biochemistry, Faculty of Health Sciences, University of Cape Town, Observatory 7925, Cape Town (South Africa)

[b] Department of Biology and Biochemistry, University of Bath, Building 4 South, Claverton Down, Bath BA2 7AY (United Kingdom), Fax: +44 1225 386779, e-mail: k.r.acharya@bath.ac.uk

Abstract. Angiotensin-converting enzyme (ACE) is a zinc- and chloride-dependent metallopeptidase that plays a vital role in the metabolism of biologically active peptides. Until recently, much of the inhibitor design and mechanism of action of this ubiquitous enzyme was based on the structures of carboxypeptidase A and thermolysin. When compared to the recently solved structures of the testis isoform of ACE (tACE) and its *Drosophila* homologue (AnCE), carboxypeptidase A showed little structural homology outside of the active site, while thermolysin revealed significant but less marked overall similarity. The ellipsoid-shaped structure of tACE, which has a preponderance of α-helices, is characterised by a core channel that has a constriction approximately 10 Å from its opening where the zinc-binding active site is located. Comparison of the native protein with the inhibitor-bound form (lisinopril-tACE) does not reveal any striking differences in the conformation of the inhibitor binding site, disfavouring an open and closed configuration. However, the inhibitor complex does provide insights into the network of hydrogen-bonding and ionic interactions in the active site as well as the mechanism of ACE substrate hydrolysis. The three-dimensional structure of ACE now paves the way for the rational design of a new generation of domain-selective ACE inhibitors.

Introduction

Angiotensin-converting enzyme (ACE, EC 3.4.15.1) belongs to the M2 family of zinc metallopeptidases and catalyses the hydrolysis of dipeptides from the carboxyl terminus of a wide variety of oligopeptides [1–4]. The most celebrated physiological substrates are angiotensin I, which is converted into the potent vasopressor angiotensin II by removal of the C-terminal His-Leu, and the vasodilator bradykinin, which is inactivated by cleavage of the penultimate Pro-Phe bond. Other substrates of ACE include gonadotropin-releasing hormone (GnRH), or luteinising hormone-releasing hormone (LH-RH); substance P; β-neoendorphin$_{1-9}$; and neurotensin, but the significance of these reactions in vivo remains uncertain. Although ACE was discovered in equine plasma almost half a century ago [5], it is only recently that its three-dimensional structure has been determined by X-ray crystallography. In this review we highlight some of the structural aspects of ACE and some of its structural homologues.

Occurrence, gene and protein organisation

ACE was initially isolated from blood plasma and largely originates from endothelial cell membranes by a proteolytic cleavage process known as shedding [6]. It represents a small fraction of the total ACE accessible to circulating angiotensin I. The enzyme has also been shown to be present in kidney and other tissues. The lungs, which are highly vascularised, are a particularly rich source, as are the testes. Human somatic ACE (sACE), comprising active N- and C-domains, is encoded by a single gene that consists of 26 exons [7]. A smaller form of ACE found only in adult testis (tACE) is encoded by the same gene, but its messenger RNA (mRNA) begins

---

* Corresponding author.

before exon 13 and continues through exon 26 [7]. Translation of this mRNA results in a 701-residue-long ACE that, except for the first 36 residues, is identical to the C-terminal domain of sACE [8].

Biological function

Angiotensin I originates from the precursor protein angiotensinogen, which is cleaved by renin, an enzyme that is released by the kidney in response to stimuli such as impaired renal blood flow, salt depletion and β-adrenergic stimulation. Activation of angiotensin I by ACE not only causes vasoconstriction through the interaction of angiotensin II with the AT_1 receptors on vascular smooth muscle cells, but also stimulates the production of aldosterone, which regulates fluid and electrolyte homeostasis [9]. Bradykinin is formed from kininogen by the action of the protease kallikrein and is inactivated by kininase I and kininase II, the latter of which is identical to ACE. Apart from its vasodilatory properties, bradykinin also has cardioprotective properties, because it promotes the formation of protective nitric oxide by the endothelium [10].

ACE substrates

ACE acts on a diverse range of substrates and displays both exopeptidase and endopeptidase activity. The substrates of this remarkable zinc metallopeptidase include the following groups: (i) biological peptides, some with known activities in vivo and others which have an uncertain destiny at physiological concentrations (reviewed in [3, 11]); (ii) shorter synthetic substrates, usually aryl oligopeptides with a blocked N-terminus, that are used for ACE activity determination; (iii) a relatively new class of N-and C-domain-specific substrates [12]; and (iv) one or two unique substrates that act as both substrate and inhibitor. The heptapeptide Ang_{1-7}, an important regulator of cardiovascular function, is a substrate for the N-domain and inhibits the C-domain of sACE. This substrate is also described later in this issue [13]. Although tACE hydrolyses most of the sACE substrates, angiotensin I is an unlikely physiological substrate for this isoform, and indeed, the substrate(s) that may be involved in tACE's role in fertility remains unknown. The use of gene targeting to disrupt the gene coding for tACE suggests that it is important for the interaction of the spermatozoa with the oviduct epithelium and the zona pellucida [14]. However, no difference in in vitro fertilization rate was observed in the presence of the potent tACE inhibitor captopril [15].

Crystal structure of human tACE

Crystallisation

Despite intensive efforts by several research groups over many years, the ACE crystal structure was only determined very recently. This has largely been due to the inability to generate ACE proteins, from natural or recombinant sources, that can yield crystals suitable for structural studies using X-ray crystallography. tACE has seven Asn-X-Ser/Thr motifs for the potential addition of N-linked oligosaccharides, and one of the main obstacles that has hampered crystallisation is the microheterogeneity of the oligosaccharides on the surface of the protein, which prevents the ordered packing of the molecule into a crystal lattice. This difficulty has been circumvented by the expression of ACE in the presence of a glucosidase I inhibitor yielding the simple, high-mannose oligosaccharides [16], and the mutagenesis of the N-linked asparagine residues to glutamine [17]. The *Drosophila* homologue of ACE (AnCE) has three N-linked glycosylation sites that are important for the stability of this homologue [18]. However, nucleation and crystal lattice formation were not adversely affected by glycosylation, and protein was isolated from high-expression Hi5 insect cells for the X-ray structure determination [19].

Overall description of the structure

The first X-ray crystal structure of human tACE and its complex with one of the most widely used inhibitors, lisinopril [N^2-[(S)-1-carboxy-3-phenylpropyl]-L-lysyl-L-proline (also known as Prinivil and Zestril)], was reported recently [20]. The structure of tACE (residues 37–625) is mainly helical with a central cavity or channel that extends for about 30 Å into the molecule (fig. 1 A). This cavity appears to divide the molecule into two 'subdomains' (fig. 1 B) [20]. The boundaries of the cavity are provided by helices α13, α14, α15, α17 and strand β4. The three N-terminal helices that cover the cavity contain several charged residues and restrict the access of large polypeptides to the active site cleft. This feature of the structure likely accounts for the enzyme's inability to hydrolyse large, folded substrates. In the native structure several ordered water molecules occupy the active site pocket, which is located deep inside the groove. Two chloride ions are bound in the interior of the structure. Residues Asp 40 (α1) and Gly 615 (four residues downstream of α20) define the N- and C-terminus of the ectodomain, respectively. This is in agreement with previous tACE mutagenesis studies [21]. All six glycosylation sites (g1–6) are distributed on the surface of the tACE molecule. The locations of different sites are shown in fig. 2.

As expected, a highly ordered zinc ion is bound at the active site (figs 1 A, 3 B). Helix α13 contains the signature
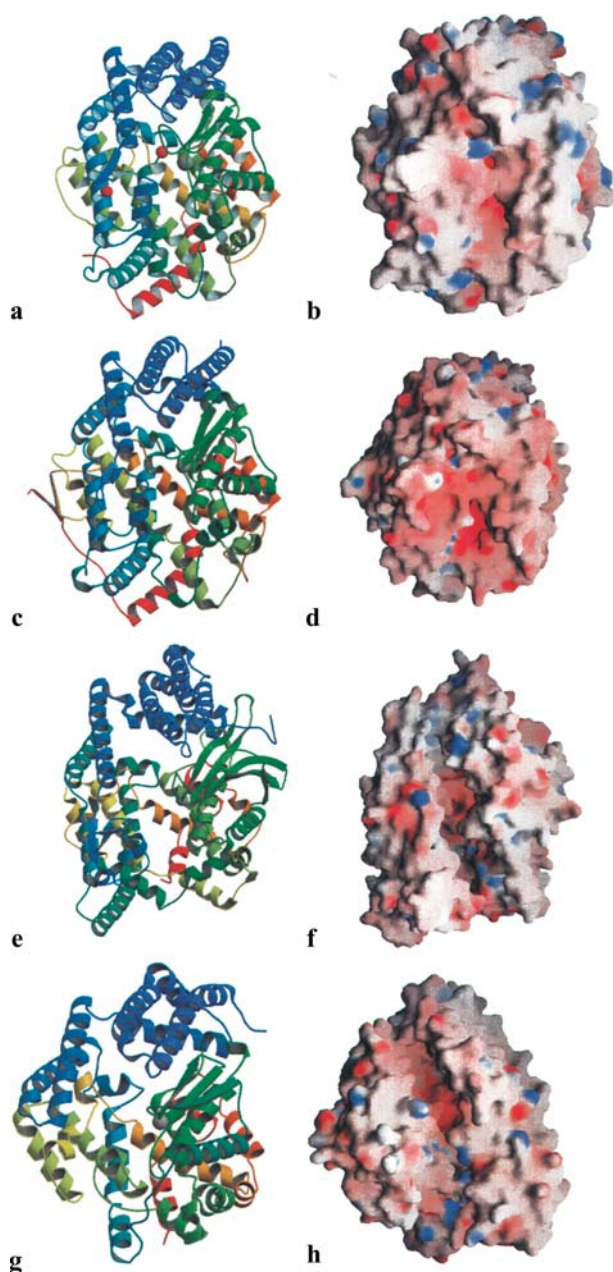
Figure 1. Ribbon and surface representation (side by side) for tACE (*a*, *b*) [20], AnCE (*c*, *d*) [19], NEU (*e*, *f*) [26], PfuCP (*g*, *h*) [27]. In the case of NEU and PfuCP, the active site forms a deep valley, while it is covered in the case of tACE and AnCE, restricting the access of substrates from the top.

HEXXH zinc binding motif, with its two zinc coordinating histidines (His 383 and His 387) [20]. In the native structure, additional coordination is provided by Glu 411 on helix α14 and an acetate ion (from the crystallisation medium). The role of a zinc ion in ACE catalysis was reported to be analogous to that in thermolysin [22] (see below).

Functional aspects

Inhibitor binding

The structure of tACE bound to the potent inhibitor lisinopril (Ki = 2.7×10^{-10} M) [23–25] shows that the inhibitor binds in a highly ordered, extended conformation, with the phenyl group extended in an N-terminal direction (fig. 3 B) and the lysine side chain parallel to the α13 helix containing the HEXXH zinc binding motif [20]. The lisinopril molecule is buried ~10 Å inside the groove. No significant rearrangement of active site residues was observed upon complex formation. The carboxyalkyl carboxylate of lisinopril is well positioned to bind to the active site zinc ion [24, 25] and provides one coordinating ligand. The position of the other three ligands (two histidines and a glutamic acid) is identical in both structures. The second oxygen atom of this carboxylate is 2.6 Å away from the zinc atom and makes a H-bond interaction with Glu 384 (OE2 atom, which appears to be protonated, as the complex was crystallised at ~pH 4.7) of the HEXXH motif [20]. The S1 phenylpropyl group makes van der Waals interactions with Val 518, and the lysyl amine forms a weak H-bond with Glu 162 (OE2 atom, 3.4 Å) at the S1′ subsite of tACE. The C-terminal carboxylate binds to Lys 511 as well as to Tyr 520.

Substrate binding

The crystal structure of tACE revealed a large central channel, with a constriction in the middle forming the active site and dividing the channel into two chambers. It is immediately apparent from inspection of the volume rendered structure that the access of substrate to the active site is severely limited. Access to the channel is only possible via a small pore in the N-terminal chamber or an occluded slot in the C-terminal chamber. An almost identical conformation is observed for the AnCE structure [19] (figs 1 C, D), and it seems likely that some flexibility in the domain movements of ACE would be required for substrate access.

Neurolysin (NEU) and carboxypeptidase from the hyperthermophilic archaeon *Pyrococcus furiosus* (PfuCP) are structural homologues of ACE, but possess a more open conformation (fig. 1 E–H) (see below). Both proteins are split into two subdomains by a large cleft [26, 27]. The active site in both enzymes is located in the interior of the cleft and about half-way along its length. ACE has been placed in the metalloprotease (zincin) superfamily because it possesses a characteristic thermolysin-like catalytic fold. Indeed, thermolysin itself is divided into two domains by a large cleft, and of particular interest is the recent observation that in the absence of substrate, thermolysin has an open conformation [28]. Comparison with the structure of the closed state demonstrates that thermolysin's two domains undergo a 5° rotation towards each other, with

Figure 2. Structure-based multiple sequence alignment along with the secondary structure. Conserved residues between tACE [20], AnCE [19], NEU [26] and PfuCP [27] are marked in black. A total of 15 residues are conserved out of which 8 residues are near the active site. Four residues, Ser 435–Gly 438, not modelled in tACE are not shown.

a

b   tACE.

c   AnCE.
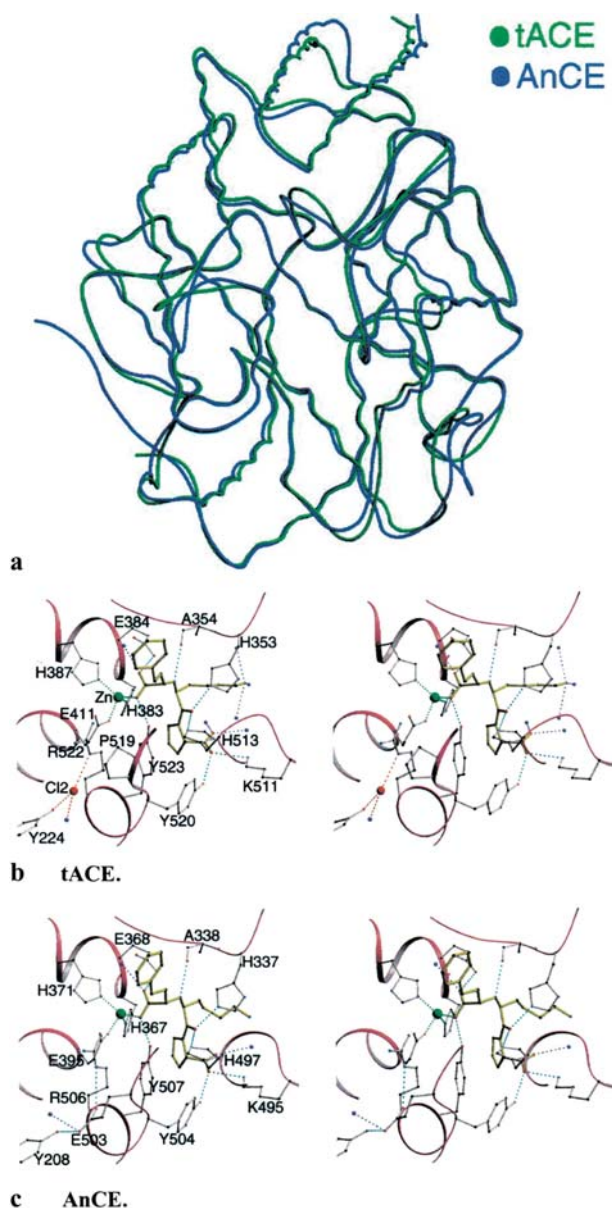
Figure 3. (*a*) C$_\alpha$ superposition of tACE and AnCE structures; (*b* and *c*) details of lisinopril binding to tACE and AnCE, respectively.

residues furthermost from the rotation axis moving by up to 3 Å. This discovery places thermolysin in the group of bacterial neutral proteases that undergo hinge-bending motions on substrate binding [29]. Considering the similarity between the active site structures of thermolysin and ACE enzymes, this level of observed flexibility suggests that ACE might exist in a more open conformation but 'close' upon substrate binding, despite the crystal structures of tACE and AnCE suggesting the contrary.

The restrictive nature of these binding clefts could significantly contribute to the specificity of peptidases, limiting their proteolytic activity to small, disordered peptides [26]. It seems likely that this is also the case for ACE.

Other oligopeptidases possess even more severe methods of substrate length restriction, despite being functionally similar [26]. Prolyl oligopeptidase and neprilysin both have large internal cavities, which substrate molecules can only access by threading through small pores, thus restricting peptidase activity to substrates lacking bulky side chains. Considering the important implications that a closed configuration holds for substrate specificity and therefore inhibitor design, the degree of flexibility present in ACE's subdomains requires further investigation. Modelling of a Phe-His-Leu tripeptide substrate for tACE with the aid of the tACE-lisinopril complex revealed a number of insights regarding the mechanism of action of tACE. The sequence and structural homology at the active site of ACE favours the mechanism of action proposed for thermolysin by Matthews [30]. The HEXXH...E residues His 383, Glu 384, His 387 and Glu 411 in tACE have their equivalent residues His 142, Glu 143, His 146 and Glu 166 in thermolysin. Ala 354 carbonyl oxygen in tACE plays a similar role to Ala 113 carbonyl oxygen in thermolysin in stabilising the scissile bond nitrogen of the substrate. The hydrolytic reaction proceeds via a general-base mechanism with the attack of a water molecule or hydroxide ion on the carbonyl carbon of the scissile bond. Stereochemical restrictions make the more direct nucleophilic attack by Glu 143 (Glu 384 in tACE) unlikely. Studies on thermolysin by Hangauer et al. [31] suggest that incoming substrate optimises its interactions with the S$_2$, S$_1$, S$_1'$ and S$_2'$ subsites by displacing the zinc-bound water toward Glu 143, resulting in polarisation between the negative carboxylate and the positive zinc. This enhances the nucleophilicity of the water oxygen, promoting attack on the carbonyl carbon. The proton accepted by the active site Glu is shuttled to the nitrogen, and as a result a tetrahedral *gem*-diolate intermediate is formed. Tyr 523 in tACE likely promotes formation of the intermediate similar to the role of His 231 and Tyr 157 in thermolysin (fig. 5). Cleavage of the C-N bond occurs with the product released in its protonated form, and again, Glu 143 in thermolysin is responsible for the abstraction of the second proton to the amine nitrogen. The terminal carboxylate of P$_2'$ is stabilised by Lys 511 and Tyr 520, while the role of Gln 281 is not clearly understood, though it forms hydrogen bond with the P$_2'$ carboxylate. Since Gln 281 appears on a protruding loop, between Leu 274 and Ile 286, which can be flexible, it may be involved in product release subsequent to hydrolysis.

Chloride activation

The activity of ACE has been shown to be activated by up to 100-fold in the presence of monovalent anions, particularly Cl$^-$ [32, 33]. This chloride requirement is both substrate and pH dependent. Hydrolysis of some substrates, such as angiotensin I, is highly chloride dependent,
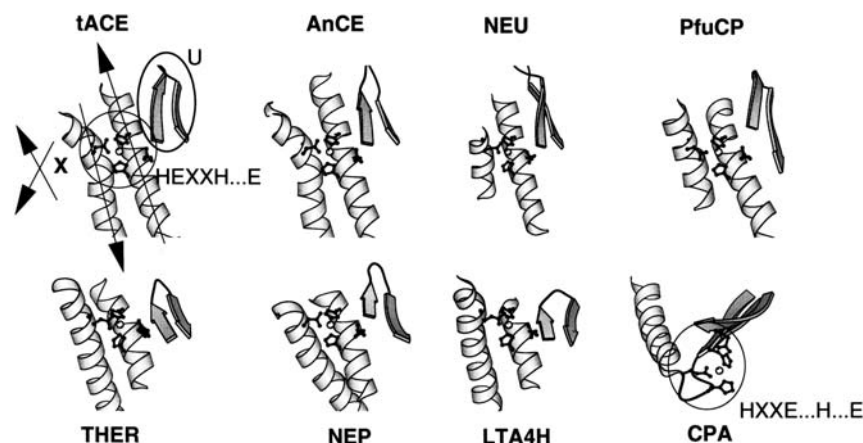
Figure 4. Active site similarity of tACE, AnCE, NEU, PfuCP, thermolysin (THER), neprilysin (NEP), leukotiene hydrolase A4 (LTA4H) and carboxypeptidase A (CPA). They all form a UX motif near the catalytic site except CPA, as depicted in case of tACE.
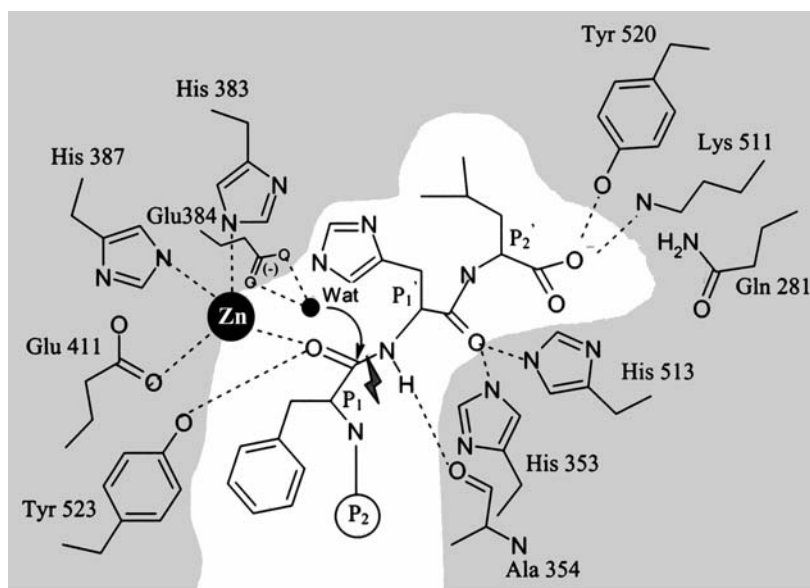
Figure 5. Details of binding of modelled tripeptide at the active site of tACE.

whereas bradykinin, for example, is hydrolysed in the absence of anion activation. Moreover, the degree of chloride activation increases with increasing pH in class I substrates where anion activation appeared to be a prerequisite for substrate binding [32, 33]. Chloride has different effects on the catalytic activity of the N and C domains of ACE, with the latter requiring much higher Cl⁻ concentrations for optimal activity [34]. The structure of tACE revealed the location of two buried chloride ions separated by 20.3 Å (fig. 1 A). The first (Cl1, 20.7 Å away from the zinc ion) is bound to four ligands, Arg 489 (NH1), Arg 186 (NE), Trp 485 (NE1) and water, and is surrounded by a hydrophobic shell of four tryptophans. The second (Cl2, 10.4 Å away from the zinc ion) is bound to Arg 522 (NE, 3.1 Å), in agreement with a previous re-

port indicating that Arg 1098 (the analogous Arg residue in the C domain of somatic ACE) is critical for the chloride dependence of ACE activity [35]. Tyr 224 and a water molecule serve as the other two Cl2 ligands. Thus, binding of each chloride ion in tACE involves ligands from both subdomains [20].

Despite knowing the exact positions of all the residues involved, the mechanism of chloride activation remains unclear. The Cl⁻ ion might restrain Arg 522 from interfering with the active site residues or, alternatively, keep the active site in a conformation that favours substrate binding. In the structure of AnCE, chloride ions are not present, despite being crystallised in the presence of 2 mM ZnCl₂ [19], yet the corresponding arginine in AnCE is in the same position as Arg 522. Interestingly, AnCE does not

possess the chloride cavity close to the active site, rather the position of the Cl2 ion in tACE (fig. 3B) is occupied by the Glu 503 residue in AnCE (fig. 3C). The loss of chloride ion interaction in case of AnCE is compensated by the two hydrogen bonds which Glu 503 makes with Arg 506 and Tyr 208.

Comparison with ACE homologues

Apart from the HEXXH zinc binding motif, there is little sequence homology between ACE and other members of the MA clan. Structural comparison of tACE with other protein structures reveals close homology with the recently determined structure of the *Drosophila* homologue of ACE (AnCE, member of the M2 family), which has ~40% amino acid sequence identity (figs 1C, D and 2) [19]. The two structures can be superimposed with an r.m.s. deviation of 1.2 Å for 571 C_α atoms (table 1, fig. 3A). In addition, the structure of AnCE in complex with lisinopril (K_i 18 nM) shows that the active sites of both tACE and AnCE have similar features, and the inhibitor binding interactions are almost identical (fig. 3B, C) (see below).

Comparison of the two structures also revealed that both tACE and AnCE exhibit significant homology with NEU [26], a protein involved in neurotensin metabolism (figs 1E, F) [36], and a newly identified carboxypeptidase from PfuCP (figs 1G, H) [27]. NEU is a member of the M3 family of oligopeptidases (member of the MA clan), and PfuCP is a member of the M32 family of carboxypeptidases. Like tACE, both belong to the family of metallopeptidases bearing the HEXXH active site motif (fig. 2) [2] and comprise an abundance of α-helices with very little β-structure (fig. 1). The two proteins exhibit little amino acid sequence similarity with tACE, yet when the two structures are optimally superimposed, there is a noticeable match, with an r.m.s. deviation of 3.9 Å for 501 C_α atoms and 3.7 Å for 427 C_α atoms against NEU and PfuCP, respectively (figs 1A, E, G; table 1). The core structures for these three proteins are similar, with significant differences in loops on the outer surface. The striking similarity also extends to the active site regions in NEU and PfuCP, which consist of deep narrow channels with ~20% larger accessible surface areas. This analysis shows that tACE, AnCE, NEU and PfuCP form a group and appear to be significantly distinct from other known metallopeptidase structures, such as carboxypeptidase A [37], thermolysin [38, 39], neprilysin [40] and leukotriene A4 hydrolase [41], even though all of them possess the conserved zinc coordinating motif at their respective active sites (fig. 4). Structurally, the catalytic zinc binding environment in all of these metallopeptidases (except in carboxypeptidase A) is composed of a conserved two helical structure [represented by motif 'X', with one helix containing the HEXXH motif and the other the 3rd zinc

Table 1. Structural alignment for tACE, AnCE, NEU, PfuCP, thermolysin and neprilysin.

RMSD Å	1J36(593)	1I1I(665)	1KA2(497)	1LNF(316)	1DMT(696)	1HS6(610)
1O86(574*)	1.2(571)	3.9(501)	3.7(427)	4.0(174)	4.0(157)	5.4(216)
1J36		3.8(502)	3.6(432)	4.7(147)	NC	4.4(154)
1I1I			3.5(445)	4.3(172)	NC	4.6(212)
1KA2				4.1(161)	4.5(154)	3.8(149)
1LNF					3.6(145)	3.5(207)
1DMT						5.4(186)
Z score						
1O86	52.1	19.3	20.6	7.5	4.5	4.6
1J36		19	20.2	6.7	NC	4.5
1I1I			19.7	6.7	NC	5.3
1KA2				5.6	3.9	4.8
1LNF					6.3	11.8
1DMT						5.3
% identity						
1O86	45	12	14	13	10	9
1J36		13	14	13	NC	8
1I1I			16	11	NC	14
1KA2				9	9	10
1LNF					17	7
1DMT						9

PDB codes: 1O86- tACE [20]; 1J36- AnCE [19]; 1I1I- NEU [26]; 1KA2- PfuCP [27]; 1LNF- thermolysin [38, 39]; 1DMT- neprilysin [40].
* Four residues disordered and hence not included.
Values in parenthesis (next to PDB code) indicate the number or residues in the protein chain and number of aligned pairs (next to individual r.m.s.values).
NC, not comparable (manual alignment, however, shows a degree of similarity near the active site).

ligand (Glu)] and an anti-parallel β-sheet structure (represented by motif 'U'), comprising a 'UX motif', which is a common feature of the gluzincins. Moreover, structural comparison of tACE with thermolysin (M4 family) revealed that there was significant, but far less striking, structural similarity between them (r.m.s. deviation of 4.0 Å for 174 C_α atoms, table 1). The study also showed that tACE has little structural similarity with carboxypeptidase A apart from the HXXE motif. The two zinc ligands in carboxypeptidase A are from this motif, and the other two additional ligands are provided by His and Glu several residues downstream from this motif in the primary sequence.

Mapping of subsite structures based on lisinopril binding to tACE and comparison with AnCE, NEU and PfuCP reveal some interesting features (fig. 2, table 2). The S_1 site is not clearly defined in tACE, as it opens up into a broad cavity. Ser 355 and Val 518 around the S_1 site form the entry residues. The S_1 site broadens by ~6 Å in the case of NEU and PfuCP as compared to tACE (taking into consideration the C_α–C_α distance between Ser 355 and Val 518 in tACE and the corresponding residues in NEU and PfuCP). The catalytic zinc binds to the carbonyl group in between the P_1 and P_1' site (fig. 5). Noticeable differences between tACE and AnCE in the vicinity of the S_1 site are the Asn 70 to Arg and Pro 519 to Glu substitutions. There are some arginine residues in the case of NEU (Arg 465, Arg 470) and PfuCP (Arg 254, Arg 261, Arg 262, Arg 311), which point towards the S_1' site, while no such residues were observed in tACE surrounding the S_1' site. Instead, negatively charged residues such as Glu 162, Glu 376 and Asp 377 surround this region. The AnCE structure portrays a similar picture to that of tACE (fig. 2, table 2). His 513 interacts with Tyr 523 OH in tACE, and the corresponding residues adopt a similar conformation in PfuCP (fig. 2, table 2). In the case of NEU, the His 601 and Tyr 613 (equivalent to His 513 and Tyr 523 in tACE) both point in the opposite direction (probably because they are free to switch over when substrate binds). Residues His 513 and His 353, though conserved in tACE, AnCE, NEU and PfuCP, appear to differ in their positioning within these structures.

Structure-based drug design of new ACE inhibitors

Over the past decade structure-based design has been used to develop drugs that target a variety of proteins, such as proteases, kinases and receptors. Notable successes include the neuraminidase inhibitors Relenza, the human immunodeficiency virus (HIV) protease inhibitor Viracept and the selective COX-2 inhibitor Rofecoxib. Within the renin-angiotensin system (RAS), renin inhibitors and aldosterone receptor antagonists have evolved using a protein structure-based approach. A growing awareness that the RAS is a far more complex regulatory system than previously recognised (reviewed in Turner and Hooper [3]); the identification of domain-specific substrates for ACE and different physiological functions of the two domains; side effects that are currently associated with ACE inhibitors; and the extensive clinical trials that have already been carried out on the first generation of ACE inhibitors provide an adequate rationale for the structure-based design of the next generation of active site-specific ACE inhibitors [42]. Moreover, the structure-based design of tACE-specific ligands to the active site and/or other regions of the germinal form of the protein may provide important insights into the role of ACE in reproductive biology.

Note. The structure-based amino acid sequence alignment was performed using the program ALSCRIPT [43]. The DALI server was used for comparison of structures [44]. The visualisation of the active site residues was performed with O [45]. Diagrams were prepared using MOLSCRIPT [46]/BOBSCRIPT [47], RASTER3D [48] and POVRAY [see http://www.povray.org]. Surface representations were prepared using GRASP [49]. Secondary structure convention was based on DSSP [50].

Table 2. Differences and similarities at the subsites S1, S1′, S2′ in tACE, AnCE, NEU and PfuCP

Subsite	Similarities and differences								
S_1	1O86 (tACE)	Ser355	Val518						
	1J36 (AnCE)	Ser339	Val502						
	1I1I (NEU)	Ala427	Tyr606						
	1KA2 (PfuCP)	Phe240	Ser416						
S1′	1O86 (tACE)	Glu162	Thr166	His353	Asn374	Glu376	Asp377	Val380	His513
	1J36 (AnCE)	Asp146	Glu150	His337	Thr358	Asp360	Gln361	Thr364	His497
	1I1I (NEU)	Tyr222	Phe226	His425	Arg465	Asp467	Glu468	Thr471	His601
	1KA2 (PfuCP)	–	–	His238	–	Arg262	Thr263	Ser266	His411
S2′	1O86 (tACE)	Gln281	Asp415	Ala418	Lys454	Phe457	Lys511	Tyr520	Tyr523	Phe527	Gln530
	1J36 (AnCE)	Gln265	Asp399	Ser402	Lys438	Phe441	Lys495	Tyr504	Tyr507	Phe511	Gln514
	1I1I (NEU)	–	Gln507	Glu510	Thr548	Leu551	Phe599	Tyr610	Tyr613	Glu617	Ser620
	1KA2 (PfuCP)	–	Arg303	Glu306	Val356	Tyr359	Asp409	Phe420	Tyr423	Thr427	Ser430

1 Ehlers M. R. and Riordan J. F. (1989) Angiotensin-converting enzyme: new concepts concerning its biological role. Biochemistry **28:** 5311–5318

2 Corvol P. and Williams T. A. (1998) Peptidyl-dipeptidase A/angiotensin I-converting enzyme. In: Handbook of Proteolytic Enzymes, pp. 1066–1076, Barrett A. J., Rawlings N. D. and Woessner J. F. (eds), Academic Press, London

3 Turner A. J. and Hooper N. M. (2002) The angiotensin-converting enzyme gene family: genomics and pharmacology. Trends Pharmacol. Sci. **23:** 177–183

4 Eriksson U., Danilczyk U. and Penninger J. M. (2002) Just the beginning: novel functions for angiotensin-converting enzymes. Curr. Biol. **12:** R745–R752

5 Skeggs L. T., Marsh W. H., Kahn J. R. and Shumway N. R. (1954) The existence of two forms of hypertension. J. Exp. Med. **99:** 275–282

6 Hooper N. M., Karran E. H. and Turner A. J. (1997) Membrane protein secretases. Biochem. J. **321:** 265–279

7 Hubert C., Houot A. M., Corvol P. and Soubrier F. (1991) Structure of the angiotensin I-converting enzyme gene. Two alternate promoters correspond to evolutionary steps of a duplicated gene. J. Biol. Chem. **266:** 15377–15383

8 Ehlers M. R., Fox E. A., Strydom D. J. and Riordan J. F. (1989) Molecular cloning of human testicular angiotensin-converting enzyme: the testis isozyme is identical to the C-terminal half of endothelial angiotensin-converting enzyme. Proc. Natl. Acad. Sci. USA **86:** 7741–7745

9 Sealey J. E. and Laragh J. H. (1990) The renin-angitensin-aldosterone system for normal regulation of blood pressure and sodium and potassium homeostasis. In: Hypertension: Pathophysiology, Diagnosis and Management, pp. 1287–1317, Laragh J. H. and Brenner B. M. (eds), Raven Press, New York

10 Henriksen E. J. and Jacob S. (2003) Modulation of metabolic control by angiotensin converting enzyme (ACE) inhibition. J. Cell. Physiol. **196:** 171–179

11 Baudin B. (2002) New aspects on angiotensin-converting enzyme: from gene to disease. Clin. Chem. Lab. Med. **40:** 256–265

12 Georgiadis D., Beau F., Czarny B., Cotton J., Yiotakis A. and Dive V. (2003). Roles of the two active sites of somatic angiotensin-converting enzyme in the cleavage of angiotensin I and bradykinin: insights from selective inhibitors. Circ. Res. **93:** 148–154

13 Ferrario C. M. and Chappell M. C. (2004) Novel angiotensin peptides. Cell. Mol. Life Sci. **61:** 2720–2727

14 Hagaman J. R., Moyer J. S., Bachman E. S., Sibony M., Magyar P. L., Welch J. E. et al. (1998) Angiotensin-converting enzyme and male fertility. Proc. Natl. Acad. Sci. USA **95:** 2552–2557

15 Metayer S., Dacheux F., Guerin Y., Dacheux J. L. and Gatti J. L. (2001) Physiological and enzymatic properties of the ram epididymal soluble form of germinal angiotensin I-converting enzyme. Biol. Reprod. **65:** 1332–1339

16 Yu X. C., Sturrock E. D., Wu Z., Biemann K., Ehlers M. R. and Riordan J. F. (1997) Identification of N-linked glycosylation sites in human testis angiotensin-converting enzyme and expression of an active deglycosylated form. J. Biol. Chem. **272:** 3511–3519

17 Gordon K., Redelinghuys P., Schwager S. L., Ehlers M. R., Papageorgiou A. C., Natesh R. et al. (2003) Deglycosylation, processing and crystallization of human testis angiotensin-converting enzyme. Biochem. J. **371:** 437–442

18 Williams T. A., Michaud A., Houard X., Chauvet M. T., Soubrier F. and Corvol P. (1996) *Drosophila melanogaster* angiotensin I-converting enzyme expressed in *Pichia pastoris* resembles the C domain of the mammalian homologue and does not require glycosylation for secretion and enzymic activity. Biochem. J. **318:** 125–131

19 Kim H. M., Shin D. R., Yoo O. J., Lee H. and Lee J. O. (2003) Crystal structure of *Drosophila* angiotensin I-converting enzyme bound to captopril and lisinopril. FEBS Lett. **538:** 65–70

20 Natesh R., Schwager S. L., Sturrock E. D. and Acharya K. R. (2003) Crystal structure of the human angiotensin-converting enzyme-lisinopril complex. Nature **421:** 551–554

21 Chubb A. J., Schwager S. L., Woodman Z. L., Ehlers M. R. and Sturrock E. D. (2002) Defining the boundaries of the testis angiotensin I-converting enzyme ectodomain. Biochem. Biophys. Res. Commun. **297:** 1225–1230

22 Soubrier F., Alhenc-Gelas F., Hubert C., Allegrini J., John M., Tregear G. et al. (1988) Two putative active centers in human angiotensin I-converting enzyme revealed by molecular cloning. Proc. Natl. Acad. Sci. USA **85:** 9386–9390

23 Wei L., Clauser E., Alhenc-Gelas F. and Corvol P. (1992) The two homologous domains of human angiotensin I-converting enzyme interact differently with competitive inhibitors. J. Biol. Chem. **267:** 13398–13405

24 Patchett A. A., Harris E., Tristram E. W., Wyvratt M. J., Wu M. T., Taub D. et al. (1980) A new class of angiotensin-converting enzyme inhibitors. Nature **288:** 280–283

25 Patchett A. A. and Cordes E. H. (1985) The design and properties of N-carboxyalkyldipeptide inhibitors of angiotensin-converting enzyme. Adv. Enzymol. Relat. Areas Mol. Biol. **57:** 1–84

26 Brown C. K., Madauss K., Lian W., Beck M. R., Tolbert W. D. and Rodgers D. W. (2001) Structure of neurolysin reveals a deep channel that limits substrate access. Proc. Natl. Acad. Sci. USA **98:** 3127–3132

27 Arndt J. W., Hao B., Ramakrishnan V., Cheng T., Chan S. I. and Chan M. K. (2002) Crystal structure of a novel carboxypeptidase from the hyperthermophilic archaeon *Pyrococcus furiosus*. Structure **10:** 215–224

28 Hausrath A. C. and Matthews B. W. (2002) Thermolysin in the absence of substrate has an open conformation. Acta. Crystallogr. D Biol. Crystallogr. **58:** 1002–1007

29 Holland D. R., Tronrud D. E., Pley H. W., Flaherty K. M., Stark W., Jansonius J. N. et al. (1992) Structural comparison suggests that thermolysin and related neutral proteases undergo hinge-bending motion during catalysis. Biochemistry **31:** 11310–11316

30 Matthews B. W. (1988) Structural basis of the action of thermolysin and related zinc peptidases. Acc. Chem. Res. **21:** 333–340

31 Hangauer D. G., Monzingo A. F. and Matthews B. W. (1984) An interactive computer graphics study of thermolysin-catalyzed peptide cleavage and inhibition by N-carboxymethyl dipeptides. Biochemistry **23:** 5730–5741

32 Bunning P. and Riordan J. F. (1983) Activation of angiotensin converting enzyme by monovalent anions. Biochemistry **22:** 110–116

33 Shapiro R., Holmquist B. and Riordan J. F. (1983) Anion activation of angiotensin converting enzyme: dependence on nature of substrate. Biochemistry **22:** 3850–3857

34 Jaspard E., Wei L. and Alhenc-Gelas F. (1993) Differences in the properties and enzymatic specificities of the two active sites of angiotensin I-converting enzyme (kininase II). Studies with bradykinin and other natural peptides. J. Biol. Chem. **268:** 9496–9503

35 Liu X., Fernandez M., Wouters M. A., Heyberger S. and Husain A. (2001) Arg(1098) is critical for the chloride dependence of human angiotensin I-converting enzyme C-domain catalytic activity. J. Biol. Chem. **276:** 33518–33525

36 Skidgel R. A., Engelbrecht S., Johnson A. R. and Erdos E. G. (1984) Hydrolysis of substance p and neurotensin by converting enzyme and neutral endopeptidase. Peptides **5:** 769–776

37 Rees D. C. and Lipscomb W. N. (1982) Refined crystal structure of the potato inhibitor complex of carboxypeptidase A at 2.5 Å resolution. J. Mol. Biol. **160:** 475–498

38 Matthews B. W., Jansonius J. N., Colman P. M., Schoenborn B. P. and Dupourque D. (1972) Three-dimensional structure of thermolysin. Nat. New Biol. **238:** 37–41

39 Matthews B. W., Colman P. M., Jansonius J. N., Titani K., Walsh K. A. and Neurath H. (1972) Structure of thermolysin. Nat. New Biol. **238:** 41–43

40 Oefner C., D'Arcy A., Hennig M., Winkler F. K. and Dale G. E. (2000) Structure of human neutral endopeptidase (Neprilysin) complexed with phosphoramidon. J. Mol. Biol. **296:** 341–349

41 Thunnissen M. M., Nordlund P. and Haeggstrom J. Z. (2001) Crystal structure of human leukotriene A(4) hydrolase, a bifunctional enzyme in inflammation. Nat. Struct. Biol. **8:** 131–135

42 Acharya K. R., Sturrock E. D., Riordon J. F. and Ehlers M. R. W. (2003) Angiotensin-converting enzyme (ACE) revisited: a new target for structure-based drug design. Nat. Rev. Drug Discov. **2:** 891–902

43 Barton G. J. (1993) ALSCRIPT: a tool to format multiple sequence alignments. Protein Eng. **6:** 37–40

44 Holm L. and Sander C. (1999) Protein folds and families: sequence and structure alignments. Nucleic Acids Res. **27:** 244–247

45 Jones T. A., Zou J. Y., Cowan S. W. and Kjeldgaard. (1991) Improved methods for building protein models in electron density maps and the location of errors in these models. Acta Crystallogr. A **47(Pt 2):** 110–119

46 Kraulis P. J. (1991) A program to produce both detailed and schematic plots of protein structures. J. Appl. Crystallogr. **24:** 946–950

47 Esnouf R. M. (1997) An extensively modified version of MolScript that includes greatly enhanced coloring capabilities. J. Mol. Graph. Model **15:** 132–134, 112–133

48 Merritt E. A. and Bacon D. J. (1997) Raster3D Photorealistic Molecular Graphics. Methods Enzymol. **277:** 505–524

49 Nicholls A., Sharp K. A. and Honig B. (1991) Protein folding and association: insights from the interfacial and thermodynamic properties of hydrocarbons. Proteins Struct. Funct. Genet. **11:** 281–296

50 Kabsch W. and Sander, C. (1983) Dictionary of protein secondary structure: pattern recognition of hydrogen-bonded and geometrical features. Biopolymers **22:** 2577–2637

To access this journal online:
http://www.birkhauser.ch